Synthesis, characterization, interaction with DNA and cytotoxicity in vitro of dinuclear Pd(II) and Pt(II) complexes dibridged by 2,2′-azanediyldibenzoic acid

ARTICLE *in* JOURNAL OF INORGANIC BIOCHEMISTRY · NOVEMBER 2008

Impact Factor: 3.44 · DOI: 10.1016/j.jinorgbio.2008.07.011 · Source: PubMed

6 AUTHORS, INCLUDING:

Mingchang Zhu
Shenyang University of Chemical Technolo…
34 PUBLICATIONS **241** CITATIONS
SEE PROFILE

Lei Liu
Sichuan University
53 PUBLICATIONS **424** CITATIONS
SEE PROFILE

Journal of Inorganic Biochemistry 102 (2008) 1958–1964

Contents lists available at ScienceDirect

Journal of Inorganic Biochemistry

journal homepage: www.elsevier.com/locate/jinorgbio

Synthesis, characterization, interaction with DNA and cytotoxicity in vitro of dinuclear Pd(II) and Pt(II) complexes dibridged by 2,2′-azanediyldibenzoic acid

Enjun Gao *, Mingchang Zhu, Hongxi Yin, Lei Liu, Qiong Wu, Yaguang Sun

Laboratory of Coordination Chemistry, Shenyang Institute of Chemical Technology, Shenyang 110142, China

ARTICLE INFO

Article history:
Received 31 January 2008
Received in revised form 20 July 2008
Accepted 21 July 2008
Available online 29 July 2008

Keywords:
Dinuclear Pd(II) and Pt(II) complexes
DNA-binding
Cleavage
Cytotoxicity in vitro

ABSTRACT

The dinuclear complexes $[Pd_2(L)_2(bipy)_2]$ (**1**), $[Pd_2(L)_2(phen)_2]$ (**2**), $[Pt_2(L)_2(bipy)_2]$ (**3**) and $[Pt_2(L)_2(phen)_2]$ (**4**), where bipy = 2,2′-bipyridine, phen = 1,10-phenanthroline and L = 2,2′-azanediyldibenzoic dianion) dibridged by H_2L ligands have been synthesized and characterized. The binding of the complexes with fish sperm DNA (FS-DNA) were investigated by fluorescence spectroscopy. The results indicate that the four complexes bound to DNA with different binding affinity, in the order complex **4** > complex **3** > complex **2** > complex **1**, and the complex **3** binds to DNA in both coordination and intercalative mode. Gel electrophoresis assay demonstrates the ability of the complexes to cleave the pBR 322 plasmid DNA. The cytotoxic activity of the complexes was tested against four different cancer cell lines. The four complexes exhibited cytotoxic specificity and significant cancer cell inhibitory rate.

1. Introduction

Cisplatin (*cis*-diamminedichloroplatinum(II)) is currently used clinically and is one of the most effective anticancer drugs in the treatment of a variety of human tumors [1,2]. Unfortunately, its usefulness limited in the development of resistance in tumor cells and the significant side effects exhibited by cisplatin have generated new areas of research, which mainly focused on the search for new metal-based complexes with low toxicity and improved therapeutic properties [3,4]. However, the researches involved direct structural analogues of cisplatin have not shown improved clinical efficacy in comparison with the parent drug, most likely because all *cis*-$[PtX_2(amine)_2]$ compounds show similar DNA-binding modes, thereby resulting in similar biological consequences. One approach to overcome this shortcoming is to identify novel materials that can be utilized as a unique class of potential anticancer agents with activity on cisplatin-resistant model systems, maybe their DNA-binding modes quite being different with that of cisplatin [5,6]. Recently, Complexes of the $[M_2(\mu\text{-}L)Y_2]$ (where M = Pd(II), Pt(II); L is a bridging ligand, and Y is an extended heterocyclic ligand) have been reported to intercalate between DNA base pairs, building blocks to behave as artificial DNA nucleases generating nicks at different DNA sites [7–10]. Furthermore, some studies show this series of complexes produce significant cytotoxic and antiproliferative effects compared with control [11].

Based on the structural analogy between Pt(II) and Pd(II) complexes, herein, we report the synthesis and characterization of the four dinuclear complexes dibridged by H_2L (L = 2,2′-azanediyldibenzoic dianion) ligands (Fig. 1). In addition, the interaction of these complexes with fish sperm DNA (FS-DNA) has been examined via fluorescence spectroscopy. Their cleavage behavior toward pBR 322 DNA and cytotoxicity in vitro were also investigated.

2. Experimental section

2.1. Materials

All chemicals and reagents purchased were of reagent grade and used without further purification unless otherwise noted. FS-DNA and pBR 322 plasmid DNA were purchased from China. The HeLa (human cervix epitheloid carcinoma) cells, the Hep-G2 (human hepatocellular carcinoma) cells, the KB (human oral epithelial carcinoma) cells and the AGZY-83a (human lung carcinoma) cells were obtained from American Type Culture Collection.

2.2. Preparation of the complexes

2.2.1. $[Pd_2(L)_2(bipy)_2]\cdot H_2O$ (**1**)

The complex was prepared as follows. A aqueous solution (10 ml) containing 1 mmol of H_2L was added dropwise into 10 ml of an water solution containing 1 mmol of $K_2[PdCl_4]$ with stirring and the mixture was allowed to react for 14 h at room temperature. Then a 10 mL ethanol solution of bipy(2,2′-Bipyridine) (1 mmol) was added and the solution was filtered and kept in air. After a few days, the resulting red crystals were obtained then filtered, washed with ethanol and dried in vacuo. Yield: 63%. Anal.

* Corresponding author. Tel.: +86 24 89385016; fax: +86 24 89388211.
E-mail address: ejgao@yahoo.com.cn (E. Gao).

0162-0134/$ - see front matter Crown Copyright © 2008 Published by Elsevier Inc. All rights reserved.
doi:10.1016/j.jinorgbio.2008.07.011

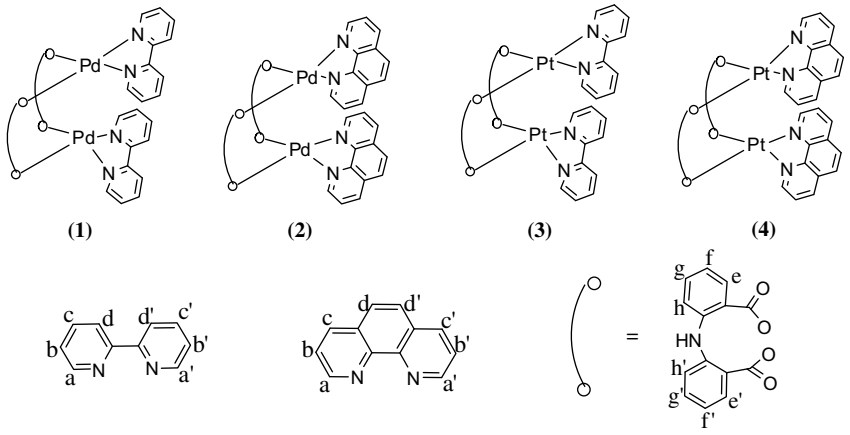

Fig. 1. Schematic structure of the four complexes and the numbering scheme for ^{1}H NMR spectroscopy.

calcd. (%) for $C_{96}H_{68}N_{12}O_{16}Pd_4 \cdot H_2O$ (**1**): C, 64.38; H, 3.38; N, 6.93. Found (%): C, 64.45; H, 3.30; N, 6.85; IR (cm^{-1}, s, strong; m, medium; w, weak): ν(O–H) 3421(m); ν(=C–H) 3083(m); ν(C=O) 1636(s); ν(C=C) 1500(s), 1452(m); ν(C–N) 1327(s); ν(C=O) 1281(m); ν(C–H) 750(m). ^{1}H NMR (DMF-d_7, 300 MHz); tt, two triplet; t, triplet; d, doublet: δ 7.48(tt, J = 7.5 Hz, 2H, Hf, Hf′), 7.86(2t, 4H, Hb, Hb′, Hg, Hg′), 7.96(d, J = 6.5 Hz, 2H, He, He′), 8.40(tt, J = 13.8 Hz, 2H, Hc, Hc′), 8.46(d, J = 6.9 Hz, 2H, Hh, Hh′), 8.70(d, J = 7.5 Hz, 2H, Ha, Ha′), 8.72(d, 2H, Hd, Hd′).

2.2.2. $[Pd_2(L)_2(phen)_2] \cdot 2H_2O$ (**2**)

This complex was synthesized in an identical manner as that described for (**1**) with phen(1,10-phenanthroline) (1 mmol,10 mL) in place of bipy. The product was obtained as a red powder. Yield: 60%. Anal. calcd. (%) for complex $C_{104}H_{68}N_{12}O_{16}Pd_4 \cdot 2H_2O$ (**2**)**:** C, 66.13; H, 3.29; N, 7.63. Found (%): C, 66.21; H, 3.21; N, 7.57. IR (cm^{-1}): ν(O–H) 3418(m); ν(=C–H) 3061(m); ν(C=O) 1621(s); ν(C=C) 1503(s), 1455(m); ν(C–N) 1335(s); ν(C=O) 1280(m); ν(C–H) 750(m). ^{1}H NMR (DMF-d_7, 300 MHz): δ 7.48(tt, 2H, Hf, Hf′), 7.56(tt, J = 7.8 Hz, 2H, Hg, Hg′), 7.79(d, 2H, He, He′), 8.01(tt, 2H, Hb, Hb′), 8.35(d, J = 9.9 Hz, 2H, Hh, Hh′), 8.52(d, J = 6.9 Hz, 2H, Hd, Hd′), 9.10(d, J = 7.01 Hz, 2H, Hc, Hc′), 9.48(d, 2H, Ha, Ha′).

2.2.3. $[Pt_2(L)_2(bipy)_2] \cdot 2H_2O$ (**3**)

This complex was synthesized in an identical manner as that described for (**1**) with $K_2[PtCl_4]$ (1 mmol,10 mL)in place of $K_2[PdCl_4]$. The product was obtained as a yellow powder. Yield: 43%. Anal. calcd (%) for complex $C_{96}H_{68}N_{12}O_{16}Pt_4 \cdot H_2O$ (**3**)**:** C, 55.03; H, 2.89; N, 6.88. Found (%): C, 55.12; H, 2.76; N, 6.81. IR (cm^{-1}): ν(O–H) 3426(m); ν(=C–H) 3083(m); ν(C=O) 1609(s); ν(C=C) 1503(s), 1452(m); ν(C–N) 1347(s); ν(C=O) 1277 (m); ν(C–H) 760(m). ^{1}H NMR (DMF-d_7, 300 MHz): δ 7.02(tt, J = 5.6 Hz, 2H, Hf, Hf′), 7.49(tt, 2H, Hb, Hb′), 7.57(tt, 2H, Hg, Hg′), 7.88(d, J = 7.125 Hz, 2H, He, He′), 8.48(m, 4H, Hc, Hc′, Hh, Hh′), 8.70(d, J = 8.1 Hz, 2H, Ha, Ha′), 9.67(d, 2H, Hd, Hd′).

2.2.4. $[Pt_2(L)_2(phen)_2] \cdot 2H_2O$ (**4**)

This complex was synthesized in an identical manner as that described for (**2**) with $K_2[PtCl_4]$ (1 mmol,10 mL)in place of $K_2[PdCl_4]$. The product was obtained as a yellow powder. Yield: 37%. Anal. calcd. (%) for complex $C_{104}H_{68}N_{12}O_{16}Pt_4 \cdot H_2O$ (**4**)**:** C, 57.36; H, 2.78; N, 6.62. Found (%): C, 57.17; H, 2.71; N, 6.73. IR (cm^{-1}): ν(O–H) 3418(m); ν(=C–H) 3058(m); ν(C=O) 1633(s); ν(C=C) 1504(s), 1463(m); ν(C–N) 1340(s); ν(C=O) 1278 (m); ν(C–H) 753(m). ^{1}H NMR (DMF-d_7, 300 MHz): δ 7.47(tt, 2H, Hf, Hf′), 7.56(tt, J = 8.1 Hz, 2H, Hg, Hg′), 7.79(d, 2H, He, He′), 8.01(tt, 2H, Hb, Hb′), 8.36(d, J = 7.52 Hz, 2H, Hh, Hh′), 8.52(d, J = 7.8 Hz, 2H, Hd, Hd′), 9.06(d, J = 6.9 Hz, 2H, Hc, Hc′), 9.48(d, 2H, Ha, Ha′).

2.3. Physical measurements

Elemental analysis (C, H and N) was performed on a model Finnigan EA 1112. The IR spectra were run as KBr pellets on Nicolet IR-470. ^{1}H NMR spectra were measured with a Bruker Avance 300 spectrometer operating at 300.13 MHz.

Fluorescence measurements were carried out on a Perkin–Elmer LS55 fluorescence spectrofluorometer. For all fluorescence measurements, the entrance and exit slits were maintained at 10 and 10 nm, respectively. The sample was excited at 526 nm and its emission observed at 602 nm. The buffer used in the binding studies was 50 mM Tris–HCl, pH 7.4, containing 10 mM NaCl. The sample was incubated 4 h at room temperature (20 °C) before spectral measurements. Under these conditions, the fluorescence intensity of the respective complexes, FS-DNA and EtBr was very small and could be ignored. The interaction of the respective Pd(II) and Pt(II) complexes with DNA in vitro was studied as described in the literature [11,12]. The measurements of EtBr binding to DNA–Pd(II)and DNA–Pt(II) complexes was studied by increase of EtBr fluorescence. The different DNA–metal complexes correspond to different values of r_f, where r_f is the formal ratio of complex to nucleotide concentration with values ranging from 0 to 3.5 in this study. Essentially, the method is considered to be titrated a given amount of DNA–metal complexes with increasing concentrations of EtBr (0.5–5 μM) and measuring the change in fluorescence intensity. The binding isotherms were obtained in the virtue of Scatchard equation [13]: $r_E/C_E = K(n - r_E)$, where K is the association constant (apparent) of the complex and n is the number of binding sites per nucleotide. C_E is the concentration of free EtBr.

For the gel electrophoresis experiments, pBR 322 plasmid DNA (0.33 μg/μL) was treated with the complexes in Tris buffer (50 mM Tris–acetate, 18 mM NaCl buffer, pH 7.2), and the contents were incubated for 1 h at room temperature. The samples were electrophoresed for 3 h at 90 V on 0.8% agarose gel in Tris–acetate buffer. After electrophoresis, the gel was stained with 1 μg/mL ethidium bromide and photographed under UV light.

2.4. X-ray crystal structure determination for the complex **1**

Single-crystal data of complex **1** were collected at 293 K the range of $1.48° < \theta < 25.02°$ on a Brucker Smart 1000 CCD diffractometer with MoKα radiation (λ = 0.71073 Å).

The structure was solved using direct methods using SHELXL 97 [14,15] and refined by full-matrix least-squares methods on F^2. All

non-hydrogen atoms were refined anisotropically. Hydrogen atoms were located from different Fourier maps. Structure solution and refinement based on 10,885 independent reflections with $I > 2\sigma(I)$ gave $R_1 = 0.0862$, $wR_2 = 0.1743$. Crystal data and structure refinement details are summarized in Table 1.

2.5. Cytotoxicity assay

The cytotoxicity of complexes was investigated on HeLa cells, the Hep-G2 cells, the KB cells and the AGZY-83a cells. The cell lines were grown in 25 cm^2 tissue culture flasks in an incubator at 37 °C in a humidified atmosphere consisting of 5% CO_2 and 95% air. The cells were maintained in logarithmic growth phase in complete medium consisting of RPMI 1640, 10% (v/v) heat-inactivated fetal calf serum, 20 mM Hepes, 0.112% bicarbonate, and 2 mM glutamine. Cell viability was assessed by the microculture tetrazollium [3-(4,5-dimethylthiazol-2-yl)-2,5-diphenyltetrazolium bromide, MTT] assay [16]. In brief, cells were seeded into a 96-well culture plate at 2×10^5 cells/well in a 100 μL culture medium. After incubation for 24 h, cells were exposed to the tested complexes of serial concentrations. The complexes were dissolved in DMF and diluted with RPMI 1640 or DMEM to the required concentrations prior to use (0.1% DMF final concentration). The cells were incubated for 72 h, followed by the addition of 20 μL MTT solution (5 mg/mL) to each well and further cultivation for 4 h. The media with MTT were removed, and 100 μL of DMSO was added to dissolve formazan crystal at room temperature for 30 min. The absorbance of each cell at 450 nm was determined by analysis with a micro plate spectrophotometer. The IC_{50} values were obtained from the results of quadruplicate determinations of at least three independent experiments.

In another trial the effect on cell growth for the four complexes was studied by culturing the cells in medium alone for 24 h, followed by 72 h treatment with 3 μg/mL concentrations. The viable cells remaining at the end of treatment period were determined by MTT assay and calculated as % of control, treated with vehicle alone (DMSO) under similar conditions.

Table 1
Crystal data and refinement for **1**

Empirical formula	$C_{96}H_{70}N_{12}O_{17}Pd_4$
Formula weight	2089.33
Temperature (K)	293(2)
Wavelength (Å)	0.71073
Crystal system	Monoclinic
Space group	$P21/n$
a (Å)	26.208(5)
b (Å)	13.701(3)
c (Å)	27.585(6)
β (deg)	93.54(3)
Volume (Å^3)	9886(3)
Z	4
D_{calc} (mg/m^3)	1.630
Absorption coefficient (mm$^{-1)}$	0.872
$F(000)$	4928
Crystal size	$0.10 \times 0.04 \times 0.02$
θ Range for data collection (deg)	1.48–25.02
Index ranges	$-30 \leqslant h \leqslant 31$, $-14 \leqslant k \leqslant 16$, $-26 \leqslant l \leqslant 32$
Reflections collected	17,350
Independent reflections (R_{int})	10,885
Data/restraints/parameters	17,350/185/1420
S	1.049
Final R indices [$I > 2\sigma(I)$]	$R_1 = 0.0862$, $wR_2 = 0.1743$
R indices (all data)	$R_1 = 0.1432$, $wR_2 = 0.1977$
Largest diffraction peak and hole (Å e^3)	1.180 and −1.011

3. Results and discussion

3.1. Crystallographic structure of complex *1*

The crystal structure of complex **1** was determined by X ray crystallography as shown in Fig. 2. Selected bond lengths (Å) and angles (deg) are shown in Table 2.

As can be seen, both Pd(II) atoms are four coordinated and each is coordinated by a bipy and dibridged by two H_2L ligands in a cofacial arrangement. The coordination geometry of both Pd atoms is square planar with rather small deviations of the ligating atoms (maximum for the Pd(1) plane 0.030 Å, for the Pd(2) plane 0.047 Å, for the Pd(3) plane 0.026 Å and the Pd(4) plane 0.052 Å)

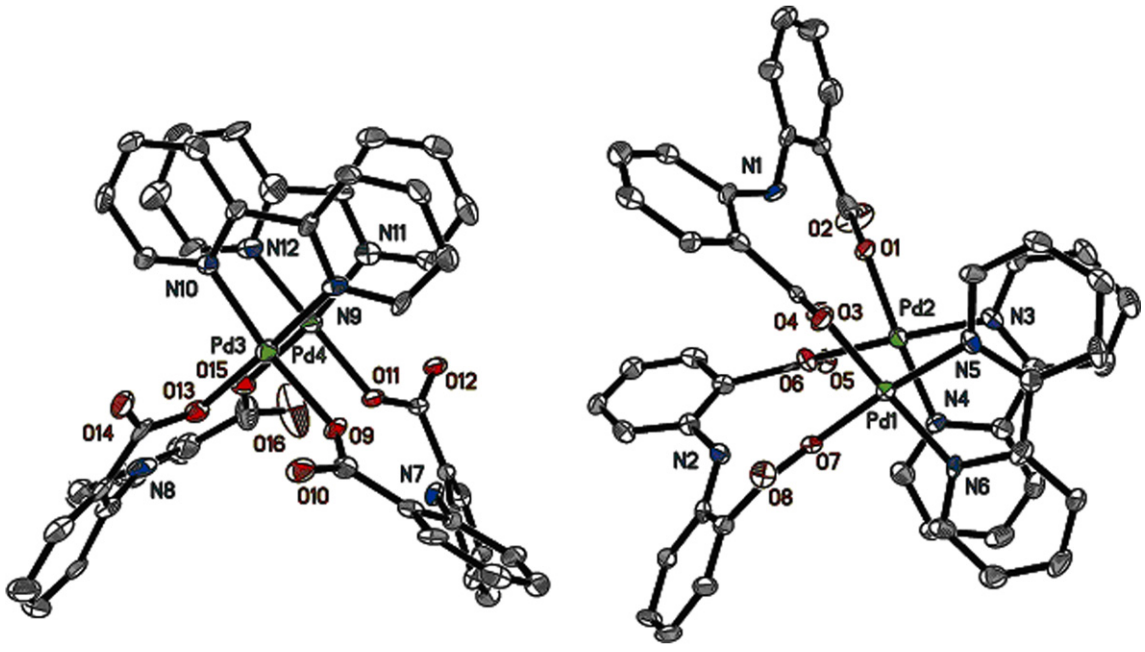

Fig. 2. The two independent molecules of **1** with numbering of atoms (H atoms were omitted for clarity) at 30% probability thermal ellipsoids.

Table 2
Selected bond lengths (Å) and angels (deg) for **1**

Pd(1)–N(6)	1.981(8)	Pd(1)–N(5)	1.999(6)
Pd(1)–O(3)	2.013(7)	Pd(1)–O(7)	2.026(5)
Pd(1)–Pd(2)	3.2423(11)	Pd(2)–N(3)	1.981(7)
Pd(2)–O(6)	1.983(5)	Pd(2)–N(4)	1.986(8)
Pd(2)–O(1)	2.028(7)	Pd(3)–N(10)	2.006(9)
Pd(3)–N(9)	2.011(7)	Pd(3)–O(9)	2.012(7)
Pd(3)–O(13)	2.014(5)	Pd(3)–Pd(4)	3.2366(11)
Pd(4)–N(11)	1.979(7)	Pd(4)–N(12)	2.002(10)
Pd(4)–O(15)	2.003(5)	Pd(4)–O(11)	2.007(7)
N(6)–Pd(1)–N(5)	81.7(3)	N(6)–Pd(1)–O(3)	177.8(2)
N(5)–Pd(1)–O(3)	96.2(3)	N(6)–Pd(1)–O(7)	92.2(3)
N(5)–Pd(1)–O(7)	172.1(3)	O(3)–Pd(1)–O(7)	90.0(2)
N(6)–Pd(1)–Pd(2)	95.09(18)	N(5)–Pd(1)–Pd(2)	96.88(18)
O(3)–Pd(1)–Pd(2)	85.85(16)	N(3)–Pd(2)–O(6)	177.6(3)
N(3)–Pd(2)–N(4)	81.4(3)	O(6)–Pd(2)–N(4)	96.6(3)
N(3)–Pd(2)–O(1)	93.8(3)	O(6)–Pd(2)–O(1)	88.0(3)
N(4)–Pd(2)–O(1)	172.9(2)	N(3)–Pd(2)–Pd(1)	85.31(18)
O(6)–Pd(2)–Pd(1)	93.27(16)	N(4)–Pd(2)–Pd(1)	88.93(18)
O(1)–Pd(2)–Pd(1)	85.50(17)	N(10)–Pd(3)–N(9)	80.8(3)
N(10)–Pd(3)–O(9)	172.9(2)	N(9)–Pd(3)–O(9)	92.4(3)
N(10)–Pd(3)–O(13)	97.3(3)	N(9)–Pd(3)–O(13)	177.3(3)
O(9)–Pd(3)–O(13)	89.6(3)	N(10)–Pd(3)–Pd(4)	93.3(2)
N(9)–Pd(3)–Pd(4)	98.99(19)	O(9)–Pd(3)–Pd(4)	85.86(17)
O(13)–Pd(3)–Pd(4)	83.04(17)	N(11)–Pd(4)–N(12)	81.6(4)
N(11)–Pd(4)–O(15)	170.6(3)	N(12)–Pd(4)–O(15)	91.2(3)
N(11)–Pd(4)–O(11)	97.5(3)	N(12)–Pd(4)–O(11)	178.4(3)
O(15)–Pd(4)–O(11)	89.6(3)	N(11)–Pd(4)–Pd(3)	84.0(2)
N(12)–Pd(4)–Pd(3)	93.0(2)	O(15)–Pd(4)–Pd(3)	90.36(18)
O(11)–Pd(4)–Pd(3)	85.64(17)		

from the coordination plane, composed of two nitrogen atoms from the bipy and two oxygen atoms from two bridging ligands. The two bridged ligands are stacked in an offset face-to-face mode arrangement by dihedral angle of 12.83° and 5.47°, conforming to an approximate π–π interaction [17] and giving rise to the value respectively Pd···Pd separation distances of 3.242 Å and 3.237 Å. The distances are similar to that double-carboxylato-bridged $(\mu\text{-}1,3\text{-}OCO)_2$ palladium complexes $\{[Pd(CH_3COO)_2]_3$, 3.105(1)–3.203(1)}[18] which reveal weak metal–metal interactions, but are longer than those in some complexes [19–21].In one lattice, the resulting distort angles of two benzene ring in L ligand (maximum of 44.79°; minimum of 35.39°) are significantly shorter than that in the L complex (45.2°). It may be noted that the strong π-acidic nature of the bipy ligands may also be considered as an additional contribution to the stabilization of the metal–metal interaction and stabilizing $(\mu\text{-}L)_2$ bridging. Therefore, the final conformation of the molecule must be the result of the sum of the different interactions. The packing structure of the complex **1** is shown in Fig. 3.

3.2. Fluorescence spectroscopic studies

Fluorescence quenching measurements can be used to monitor metal binding [22]. The molecular fluorophore EtBr emits intense fluorescence in the presence of FS-DNA due to its strong intercalation between the adjacent DNA base pairs. It was previously reported that quenching of DNA–EtBr fluorescence by the addition complexes causes a reduction in the emission intensity, indicating the competition between the complex between EtBr in binding to DNA [23]. The study involves the addition of the complexes to DNA pretreated with EtBr ([DNA]/[EtBr] = 5) and the measurement of the intensity of emission. The emission spectra of EtBr bound to DNA in the absence and presence of the four complexes are shown in Fig. 4. The addition of each Pd(II) and Pt(II) complex to DNA-bound EtBr all causes an appreciable reduction in fluorescence intensity, resulting in a decrease of the binding consent of EtBr to DNA.

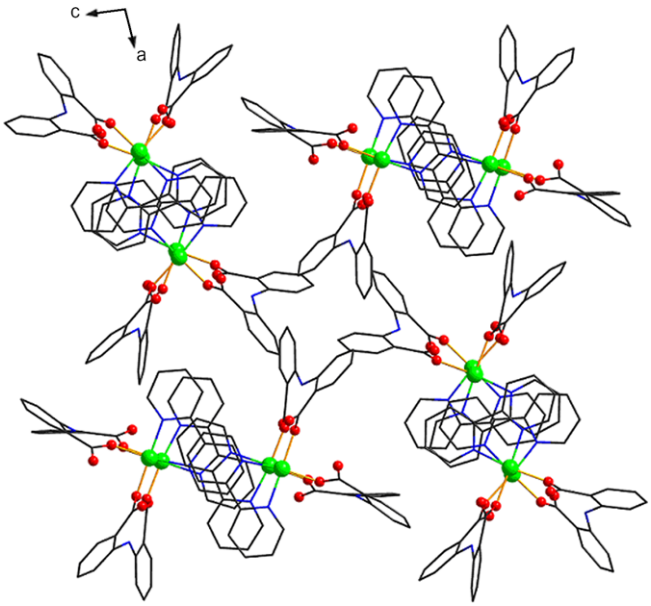

Fig. 3. Packing structure of **1** (H atoms were omitted for clarity).

According to the classical Stern–Volmer equation [24]: $I_0/I = 1 + K_{sq}r$, *where* I_0 and I represent the fluorescence intensities in the absence and presence of the complex, respectively, and r is the concentration ratio of the complex to DNA. K_{sq} is a linear Stern–Volmer quenching constant dependent on the ratio of the bound concentration of EtBr to the concentration of DNA. The K_{sq} value is obtained as the slope of I_0/I versus r linear plot. The fluorescence-quenching curve of DNA-bound EtBr by the four complexes is given in Fig. 5. The quenching curves illustrate that the complexes bind to DNA in the series of K_{sq} **4** > K_{sq} **3** > K_{sq} **2** > K_{sq} **1**. The data also indicates that the intercalary ability of the coordinated ligands varies as phen > bipy in this series of complexes [25]. Furthermore, the Pt(II) complexes have the better effect than Pd(II) on the fluorescence intensity of EtBr–DNA being quenched. Obviously, the result follows the order of complex **4** > complex **3** > complex **2** > complex **1**. Thus, it can be confirmed that the reactions of the four intercalary complexes between the adjacent DNA base pairs have taken place [26].

The fluorescence Scatchard plot is an important tool to obtain how the complexes binding to FS-DNA, which can provide the binding mode of the complexes to DNA [27]. The fluorescence Scatchard plots obtained for competition of the complex **3** with the EtBr to bind with DNA are given in Fig. 6. The complex **3** does not exhibit a typical type A or D behavior (type A behavior is considered that the slope decreases in the present of increasing amount of metal complex, with no change in the intercept on the abscissa. Type D behavior has the Scatchard plot shifted only on the abscissa but not the slope [27]). Thus, it does not show typical competitive or noncompetitive inhibition of EtBr binding for both the slope, i.e. K_{obs} (the observed association constant), and the intercept of the abscissa, i.e. n (number of binding sites per nucleotide) change with the increase in the concentrations of the complex **3** as given in Fig. 6 and Table 3. The data proves that the complex **3** may bind to DNA by both coordination binding and the intercalative binding mode.

3.3. Cleavage of pBR 322 DNA by complexes

The degree to which the four complexes could function as DNA-cleavage agents was examined using supercoiled pBR 322 plasmid

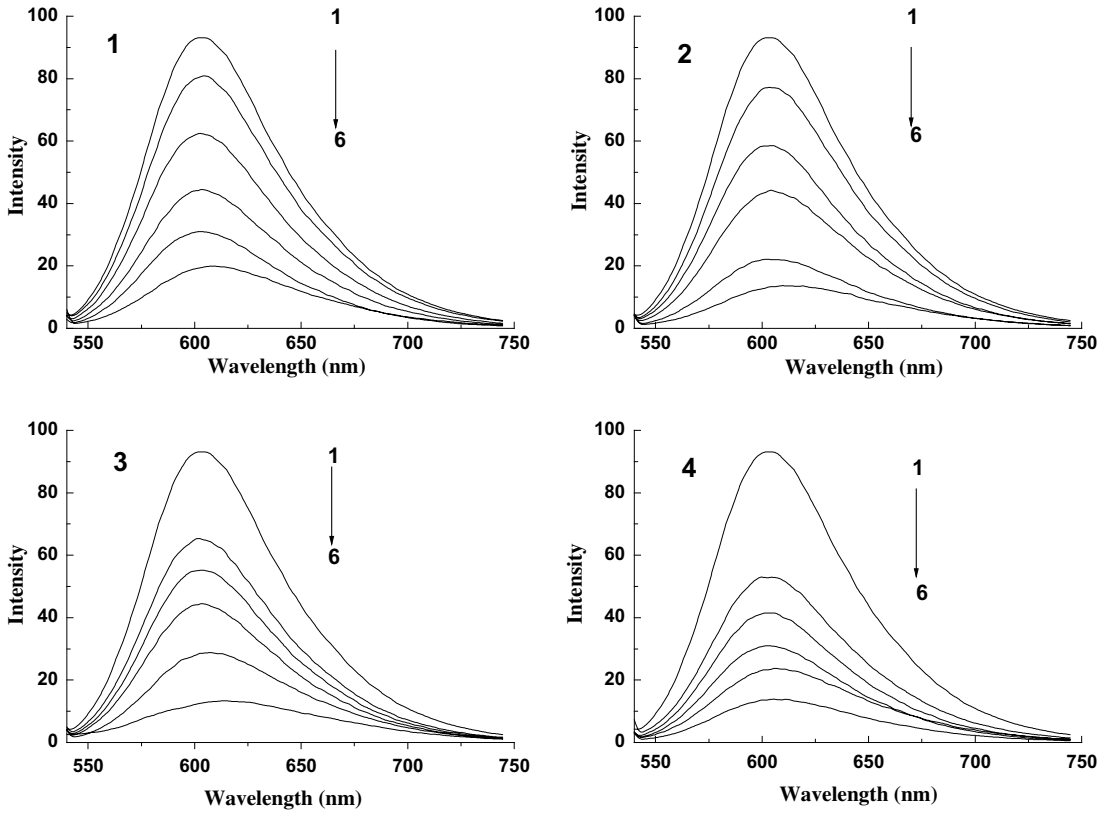

Fig. 4. Fluorescence spectra of the binding of EtBr to DNA in the absence (line 1) and presence (line 2–6) of increasing amounts of the complexes λ_{ex} = 526 nm, C_{EB} = 1.0 μM, C_{DNA} = 5.1 μM, $C_{M(1-4)}$ (line 2–6): 2.5, 5.0, 7.5, 12.5, 25 (μM).

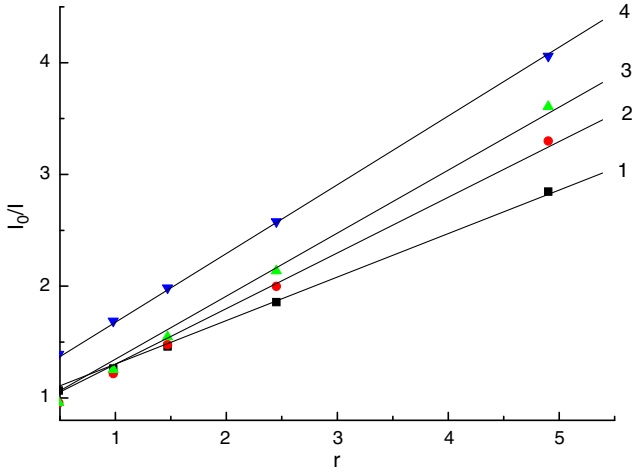

Fig. 5. Stern–Volmer quenching plots of the complex **1**, **2**, **3**, **4** with the value of slope 0.389 (complex **1**), 0.478 (complex **2**), 0.563 (complex **3**), 0.615 (complex **4**).

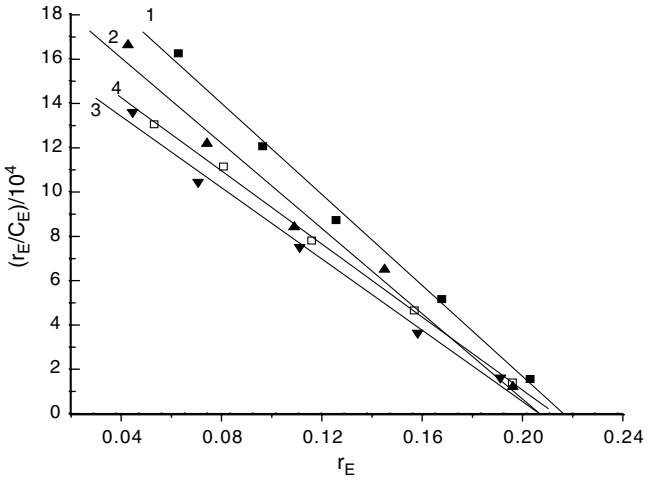

Fig. 6. Fluorescence Scatchard plots for the binding of EtBr (0.5–5 μM) to DNA in the absence (line 1) and the presence (lines 2–4) of increasing concentrations of the complex **3**. r_f increases in the order of 0.114, 1.084 and 2.201 for lines 2–4, respectively (r_f is the formal ratio of metal complex to nucleotide concentration, r_E is the ratio of bound EtBr to total nucleotide concentration).

DNA as the target. The efficiency of cleavage of these molecules was probed using agarose gel electrophoresis [28,29]. Complexes **1**, **2**, **3** and **4** were found to promote the cleavage of pBR 322 plasmid DNA from supercoiled Form (I) to the nicked Form (II) (Fig. 7). A little DNA-cleavage was observed for the control in which metal complex was absent (lane 0). The complexes **c**an induce the obvious cleavage of the plasmid DNA at the concentration of 3.3 μM. With increasing concentration of the four complexes (lanes 1–6), the amount of Form I of pBR 322 DNA diminished gradually, whereas Form II increased. On the other hand, the complexes exhibited different cleaving efficiency for the plasmid DNA. Under comparable experimental conditions, Pt(II) complexes exhibit more effective DNA-cleavage activity than Pd(II) complexes. The different DNA-cleavage efficiency of the complexes may be due to the different binding affinity of the complexes to DNA [30–33].

Table 3
Binding parameters for fluorescence Scatchard plot of FS-DNA with EtBr in the presence of **3**

r_f	K_{obs} ($\times 10^5$ M^{-1})	n
0.000	9.732	0.216
0.114	9.588	0.208
1.084	8.030	0.208
2.201	7.892	0.213

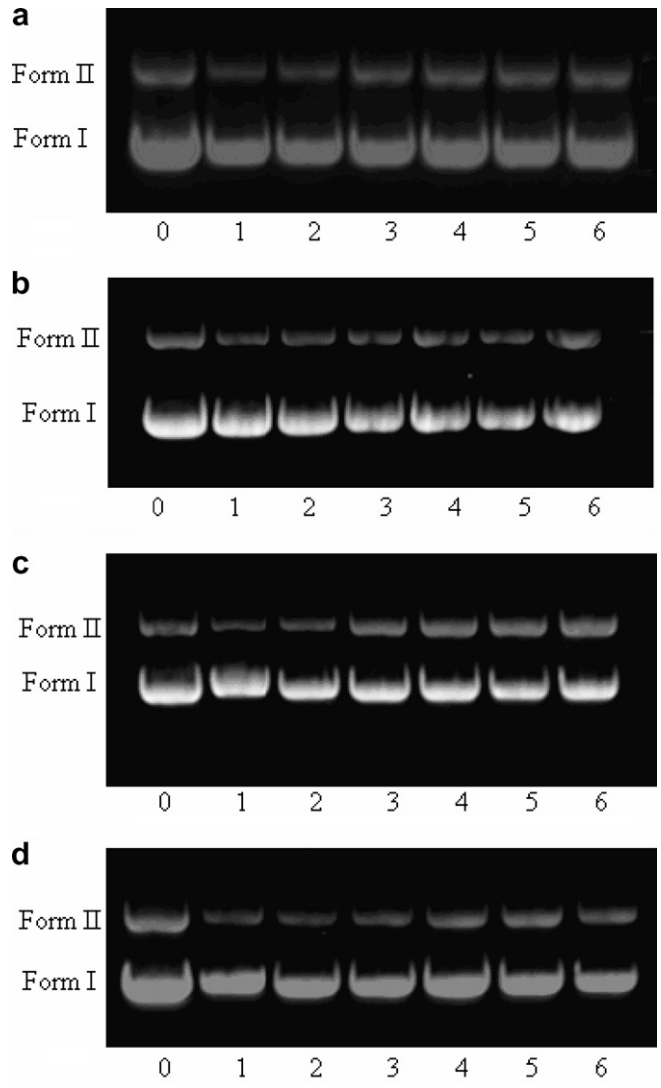

Fig. 7. Cleavage of pBR 322 DNA (10 μM) in the presence of complexes, Lane 0, DNA alone; (lanes 1–6) in the different concentrations of the complex: (1) 3.3; (2) 6.6; (3) 13.2; (4) 6.4; (5) 52.8; (6) 105.6 μM (a: complex **1**, b: complex **2**, c: complex **3**, d: complex **4**).

3.4. Cytotoxicity in vitro study

We have performed in vitro cytotoxicity tests for four complexes using selected human tumor cell lines. The IC_{50} values are listed in Table 4. In addition, Fig. 8 reveals the effect on cell growth after a treatment period of 72 h treatment with 3 μg/mL concentration.

Among the compounds studied here, the complex **4** is the most cytotoxic in all the four cell lines tested while the complex **1** is the least. The Pt(II) complexes were consistently more active than Pd(II) conjugate analogues, especially against KB cells, exhibiting

Table 4
Cytotoxicity of the complexes against selected human tumor cells after 72 h of incubation

Tumor cells	In vitro activity (IC_{50} ± SD, μM)				
	Complex **1**	Complex **2**	Complex **3**	Complex **4**	Cisplatin
Hela	6.41 ± 1.29	4.25 ± 1.67	1.23 ± 0.24	1.11 ± 0.21	0.56 ± 0.07
Hep-G2	4.14 ± 1.05	3.92 ± 0.95	2.63 ± 0.54	2.52 ± 0.53	1.61 ± 0.41
KB	3.83 ± 0.72	2.42 ± 0.39	1.62 ± 0.35	1.39 ± 0.51	1.32 ± 0.24
AGZY-83a	8.67 ± 1.93	6.47 ± 1.52	4.53 ± 0.81	3.64 ± 0.84	1.92 ± 0.42

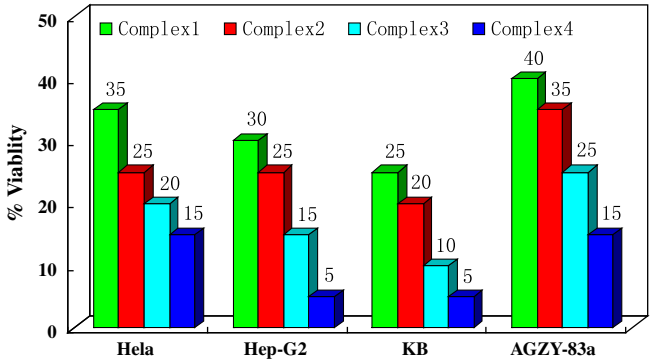

Fig. 8. Effect of 3 μg/mL of the complex on breast cancer cells viability after 72 h of incubation. All determinations are expressed as percentage of the control (untreated cells).

a high level of resistance against conventional chemotherapeutic agents. A viability rate by day 3 to less than 50% of the control values was observed for the complexes. The complexes were more effective in arresting the growth of KB than other lines. The results coincide with IC_{50} values reveals.

4. Conclusions

Four novel dinuclear complexes dibridged by H_2L ligands were synthesized and characterized. The DNA-binding properties of the complexes were examined by fluorescence spectra. The results support the fact that the complexes bind to DNA with different binding affinity. The capability of cleavage of pBR 322 DNA by the complexes was investigated using agarose gel electrophoresis and the results indicate that all complexes exhibit an efficient DNA-cleavage. Cytotoxic and antiproliferative studies show that the four complexes exhibit good cytotoxic activity against different cell lines tested in general, especially more effective against KB cell lines.

5. Abbreviations

Bipy	2,2′-bipyridine
Phen	1,10-phenanthroline
L	2,2′-azanediyldibenzoic dianion
FS-DNA	fish sperm DNA
Cisplatin	*cis*-diamminedichloroplatinum(II)
HeLa	human cervix epitheloid carcinoma cells
Hep-G2	human hepatocellular carcinoma cells
KB	human oral epithelial carcinoma cells
AGZY-83a	human lung carcinoma cells
EtBr	ethidium bromide
DMF	dimethyl formamide
MTT	tetrazollium [3-(4,5-dimethylthiazol-2-yl)-2,5-diphenyl-tetrazolium bromide
DMSO	dimethyl sulfoxide

Acknowledgements

We gratefully acknowledge the Natural Science Foundation of China (No. 20671064), the Natural Science Foundation of Liaoning Province (No. 20052014), Foundation of Educational Department of Liaoning Province (No. 20060679), and Foundation of Liaoning Bai Qian Wan Talents Program (No. 2008921054).

References

[1] B. Rosenberg, in: H. Sigel (Ed.), Metal Ions in Biological Systems, vol. II, Marcel Dekker, New York, 1980, p. 127.
[2] J. Reedijk, Inorg. Chim. Acta 198 (1992) 873–881.
[3] S.E. Sherman, S.J. Lippard, Chem. Rev. 87 (1987) 118–1153.
[4] J. Reedijk, Pure Appl. Chem. 59 (1987) 181–186.
[5] M. Miernicka, A. Szulawska, M. Czyz, I. Lorenz, P. Mayer, B. Karwowski, E. Budzisz, J. Inorg. Biochem. 102 (2008) 157–165.
[6] G. Zhao, H. Lin, Curr. Med. Chem. Anticancer Agents 5 (2005) 137–147.
[7] S.Y. Yu, M. Fujita, K. Yamaguchi, J. Chem. Soc., Dalton Trans. (2001) 3415–3416.
[8] J.W. Suggs, M.J. Dube, M. Nichols, J. Chem. Soc., Chem. Commun. (1993) 307–309.
[9] J.W. Suggs, J.D. Higgins, R.W. Wagner, J.T. Millard, in: Metal–DNA Interactions, American Chemical Society, Washington, 1989 (Chapter 10).
[10] E.M. Lempers, A. Rarilla, M. Suh, N.M. Kostic, in: T.D. Tullius (Ed.), Book of Abstracts Division of Inorganic Chemistry, National Meeting Spring, American Chemical Society, Washington, DC, 1991.
[11] R. Mital, T.S. Srivastava, J. Inorg. Biochem. 40 (1990) 111–120.
[12] R. vital, T.S. Srivastava, H.K. Parekh, M.P. Chitnis, J. Inorg. Biochem. 41 (1991) 93–103.
[13] G. Scatchard, Ann. N.Y. Acad. Sci. 51 (1949) 660–667.
[14] G.M. Sheldrick, SHELXS 97, Program for Crystal Structure Solution, University of Göttingen, Göttingen, Germany, 1997.
[15] G.M. Sheldrick, SHELXS 97, Program for Crystal Structure Refinement, University of Göttingen, Göttingen, Germany, 1997.
[16] M.C. Alley, D.A. Scudiero, A. Monks, M.L. Hursey, M.J. Czerwinski, D.L. Fine, B.J. Abbott, J.G. Mayo, R.H. Shoemaker, M.R. Boyd, Cancer Res. 48 (1988) 589–601.
[17] C. Janiak, J. Chem. Soc., Dalton Trans. 24 (2000) 3885–3896.
[18] A.C. Skapski, M.L. Smart, J. Chem. Soc., Dalton Trans. 11 (1970) 658–659.
[19] J.A.R. Navarro, M.A. Romero, J.M. Salas, J. Chem. Soc., Dalton Trans. 6 (1997) 1001–1006.
[20] M.R. Churchill, R. Mason, Nature 204 (1964) 777.
[21] W. Micklitz, W.S. Sheldrick, B. Lippert, Inorg. Chem. 29 (1990) 211–216.
[22] B.S. Yang, J.Y. Feng, Y.Q. Li, F. Gao, Y.Q. Zhao, J.L. Wang, J. Inorg. Biochem. 96 (2003) 416–424.
[23] B.C. Baguley, M. Le Bret, Biochemistry 23 (1984) 937–943.
[24] J.R. Lakowicz, G. Weber, Biochemistry 12 (1973) 4161–4170.
[25] Smita Ghosh, Archika C. Barve, Anupa A. Kumbhar, Avinash S. Kumbhar, Vedavati G. Puranik, Prasanna A. Datar, Uddhavesh B. Sonawane, Rajendra R. Joshi, J. Inorg. Biochem. 100 (2006) 331–343.
[26] H. Arakawa, R. Ahmad, M. Naoui, H.-A. Tajmir-Riahi, J. Biol. Chem. 274 (2000) 10150–10153.
[27] M. Howe-Grant, K.C. Wu, W.R. Bauer, S.J. Lippard, Biochemistry 15 (1976) 4339–4346.
[28] A.A. Holder, S. Swavey, K.J. Brewer, Inorg. Chem. 43 (2004) 303–308.
[29] F. Gao, H. Chao, F. Zhou, Y.X. Yuan, B. Peng, L.N. Ji, J. Inorg. Biochem. 100 (2006) 1487–1494.
[30] E.J. Gao, K.H. Wang, X.F. Gu, Y. Ying, Y.G. Sun, W.Z. Zhang, H.X. Yin, Q. Wu, M.C. Zhu, X.M. Yan, J. Inorg. Biochem. 101 (2007) 1404–1409.
[31] Q.L. Zhang, J.G. Liu, J.Z. Liu, H. Li, Y. Yang, H. Xu, H. Chao, L.N. Ji, Inorg. Chim. Acta 339 (2002) 34–40.
[32] X.L. Wang, H. Chao, H. Li, X.L. Hong, Y.J. Liu, L.F. Tan, L.N. Ji, J. Inorg. Biochem. 98 (2004) 1143–1150.
[33] J. Qian, W. Gu, H. Liu, F.X. Gao, L. Feng, S.P. Yan, D.Z. Liao, P. Cheng, Dalton Trans. 10 (2007) 1060–1066.